

EFIT Tutorial

Equilibrium Reconstruction Methods and Best Practices

Presented by

L.L. Lao¹ for the EFIT Team

San Diego, CA
May 29, 2013

¹General Atomics, San Diego, CA U.S.A.



Outline / Summary

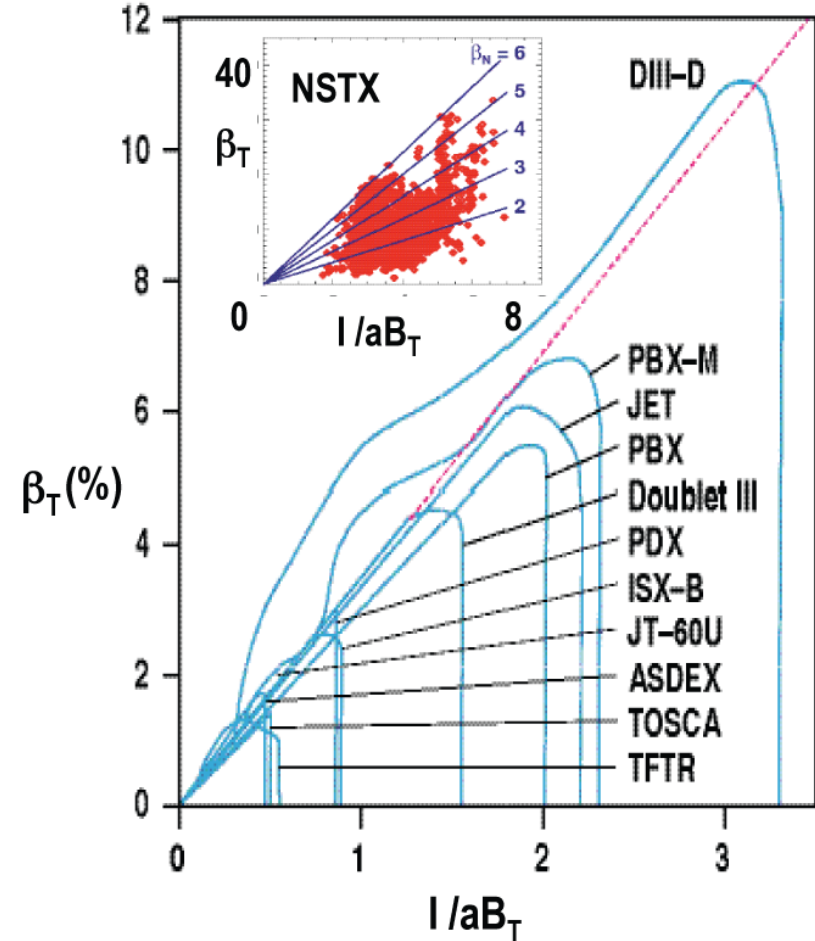
- Equilibrium reconstruction is an important component of tokamak data analysis and modeling
- EFIT reconstruct 2D tokamak equilibrium by solving the GS equation while approximately conserving experimental measurements
- EFIT efficiently searches for the solution vector by transforming the nonlinear optimization problem into a sequence of linear problems using a response function formalism and a Picard algorithm
- Amount of reconstructed information increases with diagnostic measurements available for reconstruction
- Internal current and kinetic profile measurements are necessary for full equilibrium reconstruction
- Proper choice of basis functions, boundary conditions, and physics constraints are essential to allow accurate reconstructions
- Current developments include use of GPU to speed up the computations and 3D extension to reconstruct perturbed equilibrium

Equilibrium Reconstruction Is a Crucial Component of Tokamak Data Analysis and Modeling

- Provide plasma shape and stored energy necessary for plasma operation and interpretation of experimental data
- Provide essential magnetic geometry and current and pressure profiles necessary for transport and stability studies
- Contribute to several major tokamak discoveries
 - Experimental verification of β scaling
 - Negative-central shear regime

Experimental verification of β scaling

Stambaugh, IAEA 1984



Strait Phys. Plasmas 1 (1994) 1415

EFIT Reconstructs Equilibrium by Solving the GS Equation While approximately Conserving Experimental Measurements

- Inverse problem **response \Rightarrow source**

$$\Delta^* \psi = -\mu_0 R J_\varphi(R, \psi)$$

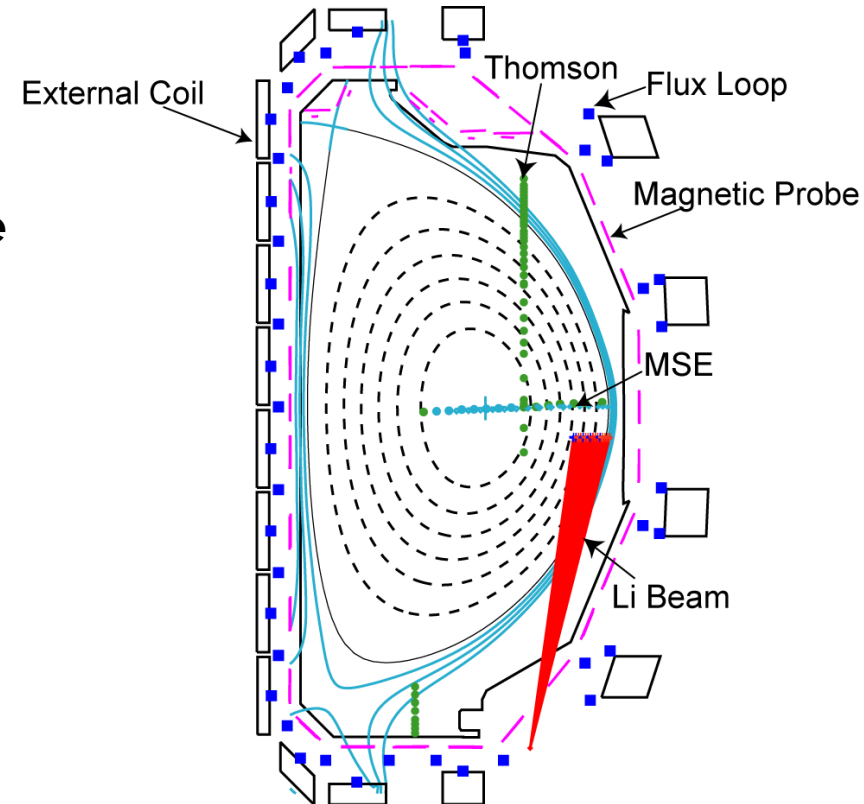
$$J_\varphi = RP'(\psi) + \frac{\mu_0 FF'(\psi)}{4\pi^2 R}$$

- Uniqueness of solution ? What information can be reconstructed ?
- Non-linear optimization problem

Measured Signals Computed Signals

$$\chi^2 = \sum_i \left(\frac{M_i - C_i}{\sigma_i} \right)^2$$

Measurement Uncertainty



Equilibrium Computed Using both Differential and Integral Forms of the GS Equation with a Picard Iteration Scheme

- Use right-handed cylindrical (R, ϕ, Z) system

$$\bar{B} = \frac{\mu_0 F(\psi)}{2\pi R} \hat{e}_\phi + \nabla\psi \times \nabla\varphi$$

- Use both differential and integral forms of the GS equation

$$\Delta^*\psi = -\mu_0 RJ_\varphi(R, \psi)$$

$$\psi(\bar{r}) = \sum_j G_\psi(\bar{r}, \bar{r}_{ej}) I_{ej} + \int_V dR' dZ' G_\psi(\bar{r}, \bar{r}') J_\varphi[R', \psi(\bar{r}')] \quad \text{Boundary Fluxes}$$

$$J_\varphi = RP'(\psi) + \frac{\mu_0 FF'(\psi)}{4\pi^2 R}$$

- Solved using Picard's iteration scheme

$$\psi = \psi_{ext} + \psi_P$$

$$\Delta^*\psi_P^{m\theta} = -\mu_0 RJ_\varphi(R, \psi^{m\theta}), \psi^{m+1} = (1 - \vartheta)\psi^m + \vartheta\psi^{m\theta}$$

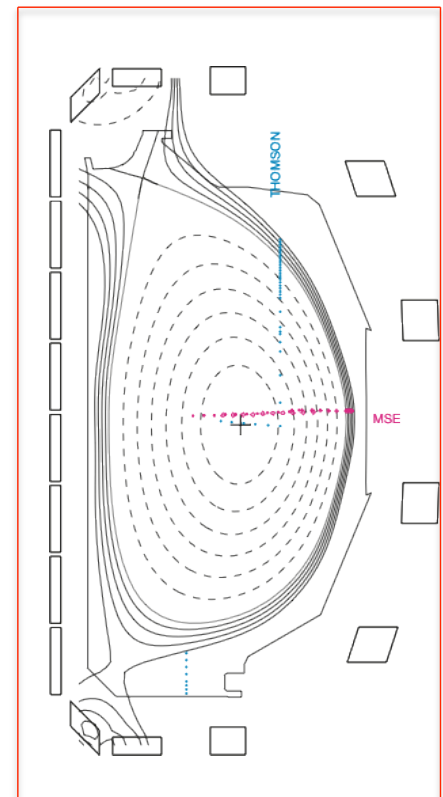
$$\psi_{ext}(\bar{r}) = \sum_j G_\psi(\bar{r}, \bar{r}_{ej}) I_{ej}$$

Convergence Error = Max | $(\psi^{m+1} - \psi^m)/\psi_{NORM}$ |

RELAX



Rectangular Computational Domain



Non-Linear Optimization Efficiently Solved by Transforming into a Sequence of Linear Problems

- Dependence on ψ linearized with the Picard iteration scheme using the integral form

$$C_i^{m+1}(\bar{r}) = \sum_j G_{C_i}(\bar{r}, \bar{r}_{ej}) I_{ej} + \int_V dR' dZ' G_{C_i}(\bar{r}, \bar{r}') J_\varphi(R', \psi^m(\bar{r}'))$$

- The plasma current source is represented in terms of a set of basis functions x_n with linear parameter vector α

$$P'(\psi) = \sum_n \alpha_n x_n$$
$$\bar{R} \bar{\alpha} = \bar{M}$$
$$FF'(\psi) = \sum_n \gamma_n x_n$$
$$\Delta^* \psi^{m+1} = -\mu_0 R J_\varphi(R, \psi^m, \alpha)$$

Measurement Vector

Type of Basis Functions
Boundary Conditions

Number of Fitting Parameters

Response Matrix

- The parameter vector α solved using the singular-value decomposition method to decompose the **response matrix** \bar{R} into a diagonal form
- Inverting Δ^* while approximately conserving the measured fluxes and magnetic fields.

$$\text{Condition Number} = \lambda_{\text{MAX}} / \lambda_{\text{MIN}}$$

EFIT Approximately Conserves Experimental Measurements and Physics Constraints Using the Response Matrix

- **Rectangular matrix**

Measurement +
Physics Constraints
Vector

$$\overline{\overline{R}} \overline{\alpha} = \overline{M}$$

Response Matrix

- **# of independent measurements \geq # of fitting parameters**
- **Solve by singular-value decomposition method to decompose the response matrix $\overline{\overline{R}}$ into a diagonal form**

Condition Number = $\lambda_{\text{MAX}} / \lambda_{\text{MIN}}$

Equilibrium and Fitting Iterations are efficiently coupled

- Iteration procedures
 - Guess J_φ , for example, $1/R$ inside an ellipse
 - Start iterations
 - ⇒ Compute I_{ej} from specified flux values at a set of flux loops
 - ⇒ Compute ψ_P at rectangular computation domain boundary using integral form of equilibrium equation
 - ⇒ Obtain ψ_P at interior points using differential form by inverting Δ^*
 - ⇒ Obtain ψ_{ext} using integral form
 - ⇒ Sum to obtain ψ everywhere
 - ⇒ Check for convergence
 - ⇒ If not, find plasma boundary enclosed by specified limiter and magnetic axis
 - ⇒ *Update fitting parameters from measurements*
 - ⇒ Compute J_φ from specified functional forms of 2 free stream functions
 - ⇒ Repeat iteration

Amount of Information That Can Be Reconstructed Increases with Availability of Diagnostics

- **External magnetics**
 - Plasma boundary, β_p , ℓ_i , and I_p
 - $\beta_p + \ell_i/2$ if circular
- **External magnetics plus MSE**
 - Plasma boundary, β_p , ℓ_i , and I_p
 - q profile, some information on internal magnetic geometry
- **External magnetics plus MSE and kinetic profiles**
 - Plasma boundary, β_p , ℓ_i , and I_p
 - q profile
 - Pressure profile and internal magnetic geometry
- **SXR, ECE**
 - Some topological and current profile information

Lao, et al. Nuc. Fusion 25 (1985) 1421

Lao, et al. Nuc. Fusion 25 (1985) 1611

Equilibrium Reconstruction Has Evolved Significantly over the Last 25 Years

EFIT

- First developed in early 1980
 - Extension of filament to distributed current source constrained by MHD equilibrium
 - DEC Array Processor, ~ 5 mins/slice
 - Successfully applied to demonstrate D-III β limit to follow Troyon scaling (IAEA 84)
- Kinetic profile, late 1980
 - Measured thermal + computed beam
- Iron core, early 1990 **JET**
- MSE and full kinetic reconstruction, early 1990
- Toroidal rotation and E_R correction, early 1990
- Real time EFIT plasma control, mid 1990 **rtEFIT**
 - Optimized C and C++, Isoflux/fixed-boundary
- Spline representation, localized current source, late 1990
- ECE isoflux and current hole constraints, early 2000
- Li beam, mid 2000
- SXR, anisotropic pressure late 2000
- GPU, 3D extensions

EFIT Algorithms and Physics Constraints

- **Lengthy Green/response function calculations are pre-computed and stored**
- **Equilibrium and fitting iterations are combined to reduce computational effort**
- **All measurements are appropriately weighted by their respective uncertainties plus a fitting weight vector**
- **Boundary constraints (Thomson, CER)**
- **Edge bootstrap current**

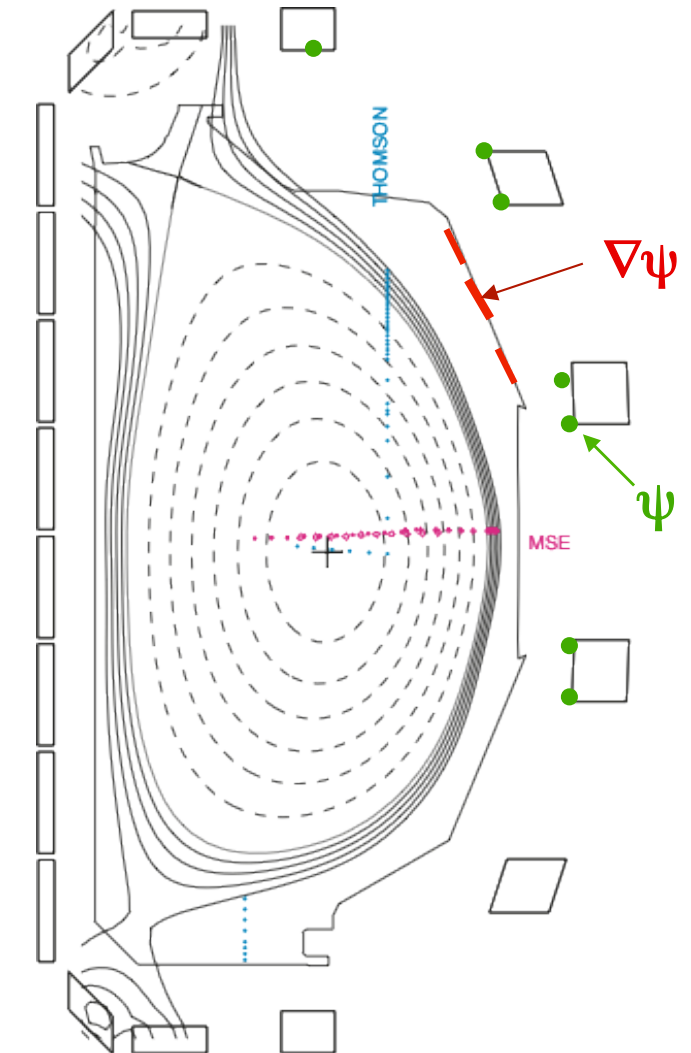
Running EFIT on Linux Stations: SNAP and Input File Modes

- Sources are under SVN
- Compile with PGF90 Fortran compiler, single CPU and MPI versions
- Running
 - /link/efit/efitd90 129 (or 65, 257,513)
 - SNAP extension mode 7 *efit_snap.dat_ext* or mode 3 *efit_snap.dat*
 - ⇒ SNAP file contains inputs needed for running
 - Make input file mode 5 *efit_snap.dat*
 - Run using input file mode 2
 - *tekx* to make plots or *efitviewer*, *EASTViewer*

IMFIT/OMFIT Integrated
Modeling Tools

Plasma Boundary Determined Magnetically by Extrapolating Magnetic Measurements Inward

- **Magnetic diagnostic measures ψ and its derivatives**
 - DIII-D 41 flux loops: ψ , 73 magnetic probes: $\nabla\psi$
- **Equilibrium relates 2nd derivatives to ψ and $\nabla\psi$**
- **Taylor series expansion to extrapolate inward to find plasma boundary**
 - More accurately determined if separatrix closer to magnetic probes and more measurements available



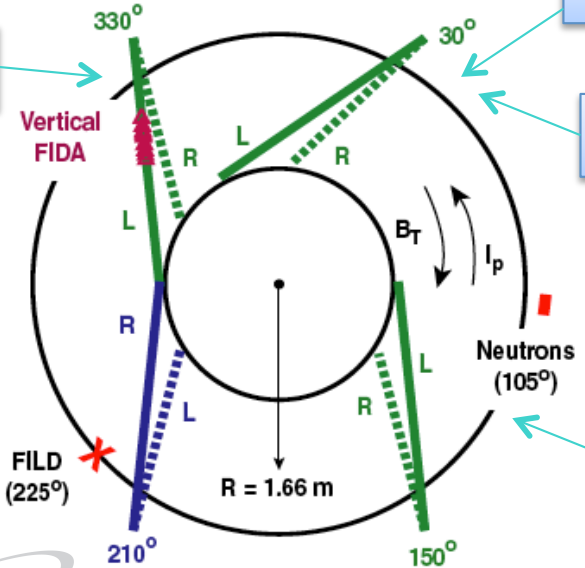
Thomson T_e Measurements Provide a Useful Indicator to Characterize Edge Magnetic Geometry and Response

- H-mode discharges only
- 3 parameters (amplitude, radius, width) TANH fit to T_e

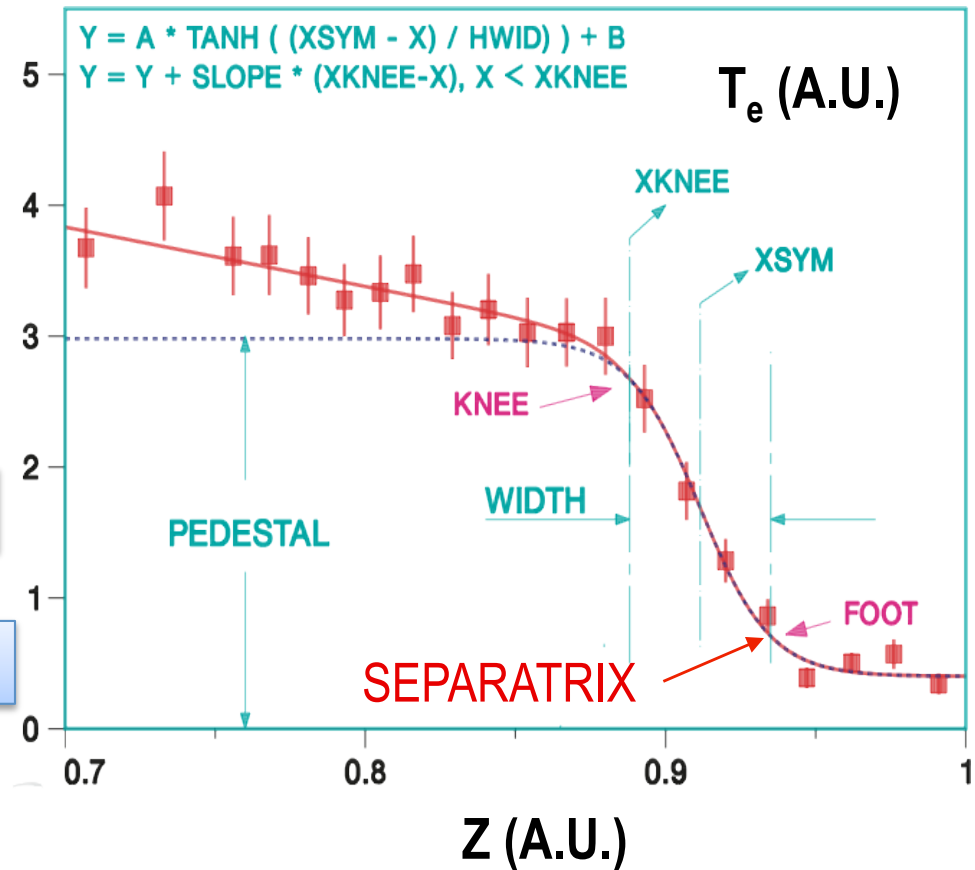
$$Z_{TS} = Z_{SYM} + 0.5 \Delta Z_{WIDTH}$$

- Previous analyses indicate some consistency with UEDGE divertor heat flux solution
- Thomson located at $\phi = -120^\circ$

Magnetics



Groebner MTANH Fit to Thomson T_e



Porter, Phys. Plasmas 5, 1410 (1998)

Various SNAP Files are Available to Accommodate Different Reconstructions

- JT: Magnetic, L- and H-mode, small finite P'(1), FF'(1), 3+ fitting parameters
- Def: Magnetic, L-mode, P'(1) = FF'(1)= 0, 3 fitting parameters

```
venusa 252: ls /link/efit/efit_snap.dat_*
/link/efit/efit_snap.dat_23      /link/efit/efit_snap.dat_iter
/link/efit/efit_snap.dat_31      /link/efit/efit_snap.dat_j
/link/efit/efit_snap.dat_31ipramp /link/efit/efit_snap.dat_jt
/link/efit/efit_snap.dat_adjw    /link/efit/efit_snap.dat_jt2
/link/efit/efit_snap.dat_circle  /link/efit/efit_snap.dat_jta_f
/link/efit/efit_snap.dat_def     /link/efit/efit_snap.dat_jta_f_old
/link/efit/efit_snap.dat_defa   /link/efit/efit_snap.dat_jta_f_tek
/link/efit/efit_snap.dat_defa_old /link/efit/efit_snap.dat_jta_t
/link/efit/efit_snap.dat_defz   /link/efit/efit_snap.dat_jta_t_old
/link/efit/efit_snap.dat_defz.old /link/efit/efit_snap.dat_jtb
/link/efit/efit_snap.dat_eredge  /link/efit/efit_snap.dat_jtdis
/link/efit/efit_snap.dat_erp    /link/efit/efit_snap.dat_jtkin
/link/efit/efit_snap.dat_erp35  /link/efit/efit_snap.dat_jt_offn1c
/link/efit/efit_snap.dat_erp36  /link/efit/efit_snap.dat_jt_pcs
/link/efit/efit_snap.dat_erp_old /link/efit/efit_snap.dat_jtramp
/link/efit/efit_snap.dat_ers    /link/efit/efit_snap.dat_jtts
/link/efit/efit_snap.dat_ers35  /link/efit/efit_snap.dat_jtv
/link/efit/efit_snap.dat_ers36  /link/efit/efit_snap.dat_jtz
/link/efit/efit_snap.dat_ers36z /link/efit/efit_snap.dat_jtzC
/link/efit/efit_snap.dat_ers_old /link/efit/efit_snap.dat_lmse
/link/efit/efit_snap.dat_ersp   /link/efit/efit_snap.dat_mse06
/link/efit/efit_snap.dat_ers_t   /link/efit/efit_snap.dat_mse07a
/link/efit/efit_snap.dat_ers_t_old /link/efit/efit_snap.dat_mse07b
/link/efit/efit_snap.dat_fp_ohless /link/efit/efit_snap.dat_mse08
/link/efit/efit_snap.dat_hipramp /link/efit/efit_snap.dat_mse08kin
/link/efit/efit_snap.dat_hy03   /link/efit/efit_snap.dat_mse08b
/link/efit/efit_snap.dat_ipramp /link/efit/efit_snap.dat_mse08z

/link/efit/efit_snap.dat_mse09
/link/efit/efit_snap.dat_mse09Er
/link/efit/efit_snap.dat_mse1
/link/efit/efit_snap.dat_mse10
/link/efit/efit_snap.dat_mse10er
/link/efit/efit_snap.dat_mse11
/link/efit/efit_snap.dat_mse12Er
/link/efit/efit_snap.dat_mse2
/link/efit/efit_snap.dat_mse2_j1
/link/efit/efit_snap.dat_msep
/link/efit/efit_snap.dat_msep16
/link/efit/efit_snap.dat_msep8
/link/efit/efit_snap.dat_mses
/link/efit/efit_snap.dat_mses16
/link/efit/efit_snap.dat_mses_er
/link/efit/efit_snap.dat_mses_time
/link/efit/efit_snap.dat_noer21
/link/efit/efit_snap.dat_noer35
/link/efit/efit_snap.dat_noer36
/link/efit/efit_snap.dat_pvac
/link/efit/efit_snap.dat_ramp
/link/efit/efit_snap.dat_revip
/link/efit/efit_snap.dat_scrape
/link/efit/efit_snap.dat_smalludn
/link/efit/efit_snap.dat_test
/link/efit/efit_snap.dat_vh
```

JT SNAP File Allows for weak Finite Edge Current Density

- JT: Magnetic, L- and H-mode, small finite $P'(1)$, $FF'(1)$
- 5 fitting parameters with 2 weak constraints => 3+

```
EFIT_SNAP.DAT_JT (rename to EFIT_SNAP.DAT for EFITD)
&efitin
  scrape=0.04      nextra=2          itek=0          icprof=3
  qvfit=0.0        fwtbp=0.           kffcur=3       kppcur=2
  fwtqa=0.00       zelip=1.0e7       iavem=5        iavev=10
  n1coil=2         nicoil = 1
  fwtsi = 44*1.0
  fwtmp2 = 76*1.
  fwtcur= 1.      nccoil=1
  ERROR = 1.E-3,   ERRMIN = 1.0E-3, MXITER=25
  FCURBD = 0.0,   PCURBD = 0.0,
  KCALPA = 1,     KCGAMA = 1,
  CALPA = 0.1  0.1  0.1      XALPA = 0.0
  CGAMA = 0.1  0.1  0.1      XGAMA = 0.0,
  iout=4
/
```

$$P'(\psi) = \alpha_0 + \alpha_1 x , \quad 0.1\alpha_0 + 0.1\alpha_1 = 0 \quad (22)$$

$$FF'(\psi) = \gamma_0 + \gamma_1 x + \gamma_2 x^2 , \\ 0.1\gamma_0 + 0.1\gamma_1 + 0.1\gamma_2 = 0 . \quad (23)$$

DEF SNAP File Forces Edge Gradients to Vanish

- Def: Magnetic, L-mode, $P'(1) = FF'(1) = 0$, 3 fitting parameters
- 3 fitting parameters

```
EFIT_SNAP.DAT_DEF (rename to EFIT_SNAP.DAT for EFITD)
&efitin
  scrape=0.04          nextra=2           itek=5           icprof=1
  qvfit=0.0             fwtpbp=1.          kffcur=2         kppcur=2
  fwtqa=0.00            zelip=1.0e7        iavem=5          iavev=10
  pcurbd=1.0            fcurbd=1.0        n1coil=0
  fwtsi = 44*1.0
  fwtmp2= 76*1.
  fwtcur= 1.            nccoil=1
  iout=4
/
```

EFIT Basis Functions: Polynomials, Tension Splines, Local Cosine, Tanh

- **Polynomials** $y_n(x) = x^n$.
- **Tension splines**

$$\begin{aligned}y_n(x) &= \frac{y_n''(x_n)}{\sigma_T^2} \left[\frac{\sinh(\sigma_T \Delta x_{n+1})}{\sinh(\sigma_T w_{n+1})} - \frac{\Delta x_{n+1}}{w_{n+1}} \right] \\&\quad + y_n(x_n) \frac{\Delta x_{n+1}}{w_{n+1}} \\&\quad + \frac{y_{n+1}''(x_{n+1})}{\sigma_T^2} \left[\frac{\sinh(\sigma_T \Delta x_n)}{\sinh(\sigma_T w_{n+1})} - \frac{\Delta x_n}{w_{n+1}} \right] \\&\quad + y_{n+1}(x_{n+1}) \frac{\Delta x_n}{w_{n+1}} , \quad x \in (x_n, x_{n+1}) , \\y_n(x) &= 0 , \quad x \notin (x_n, x_{n+1}) .\end{aligned}\tag{16}$$

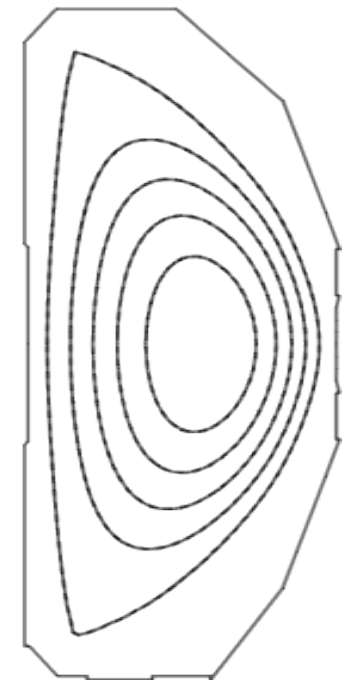
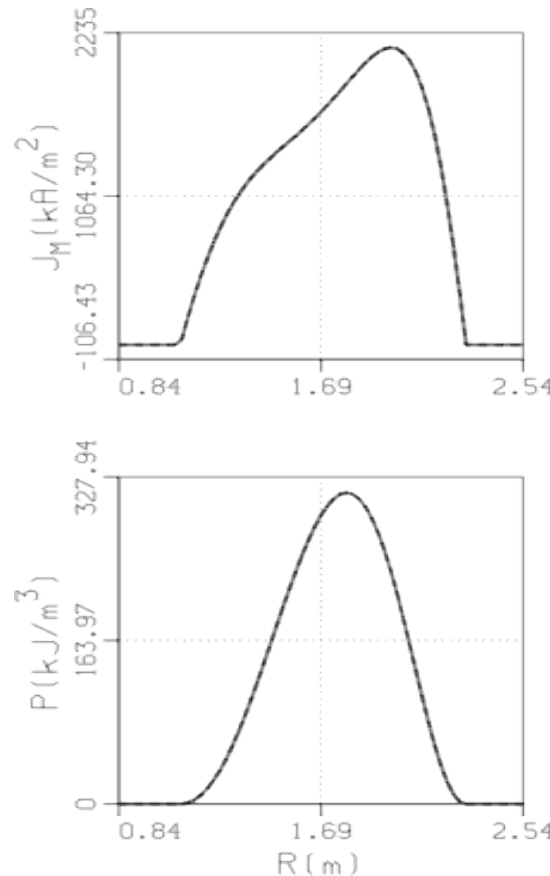
- **Local Cosine Square**

$$\begin{aligned}J_\phi(R, \psi) &= J_{\phi 0}(R, \psi) + J_{local}(R, \psi) , \\J_{local} &= \gamma_{local} \frac{\cos^2 k\tilde{x}}{R} , \quad |\tilde{x}| \leq 1 ,\end{aligned}$$

Benchmark and Consistency Tests Are Important Parts of Equilibrium Reconstruction

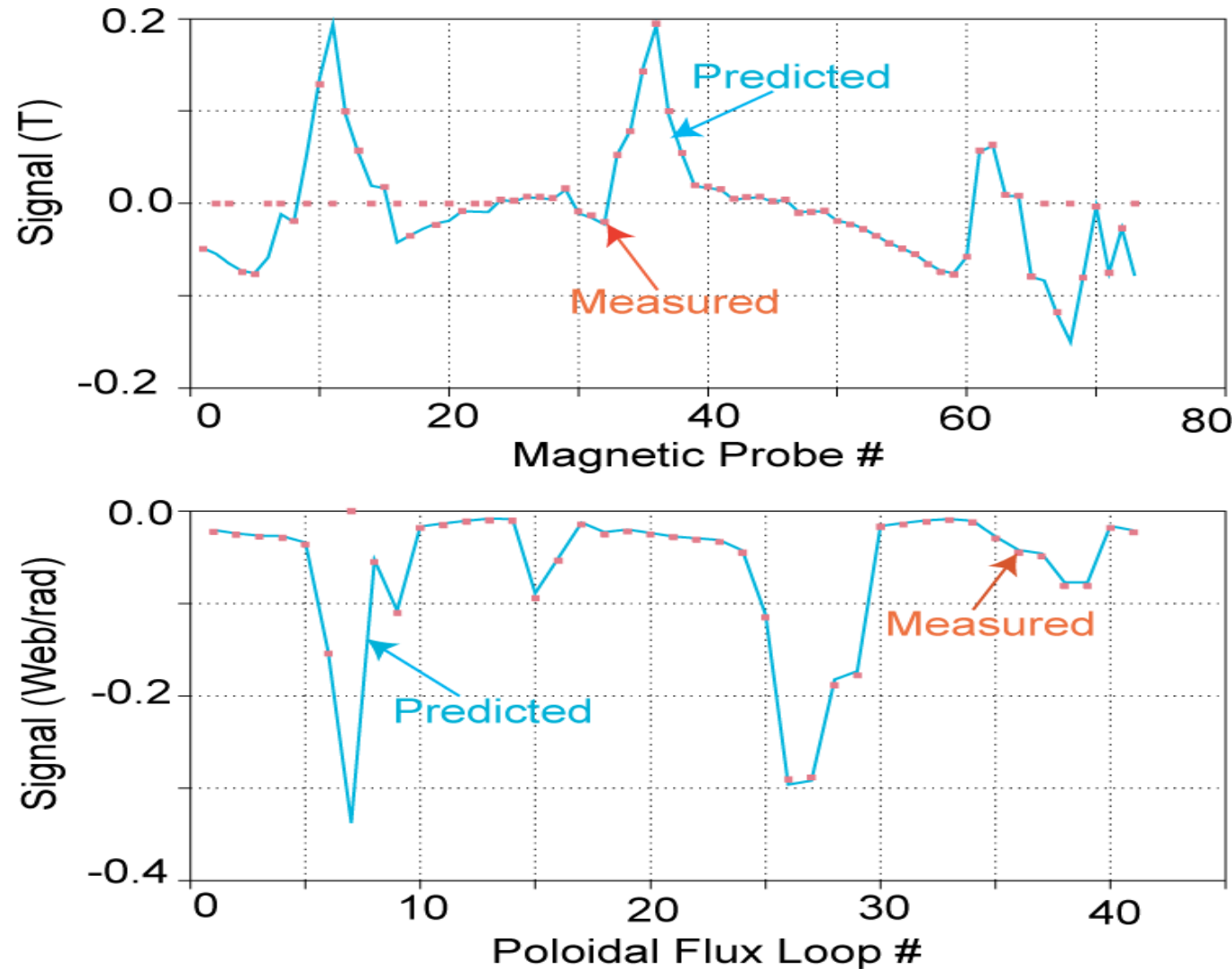
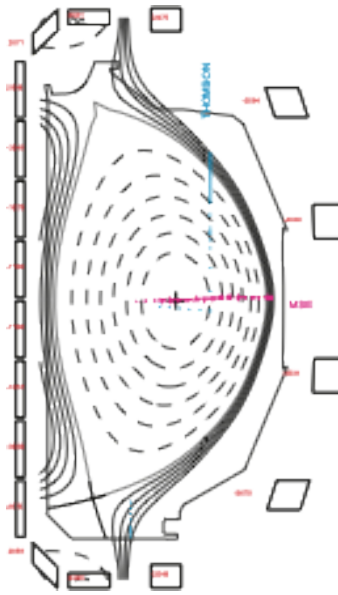
- Analytic Solovev equilibria
- Consistency between fixed and free boundary solutions
- Reconstructions using simulated signals
- Vacuum testing of magnetic probe and flux loop signals
- Consistency among different diagnostics
- Local and global force balance
- Acceptable fitting quality χ^2

— Reconstructed
..... Initial Equilibrium



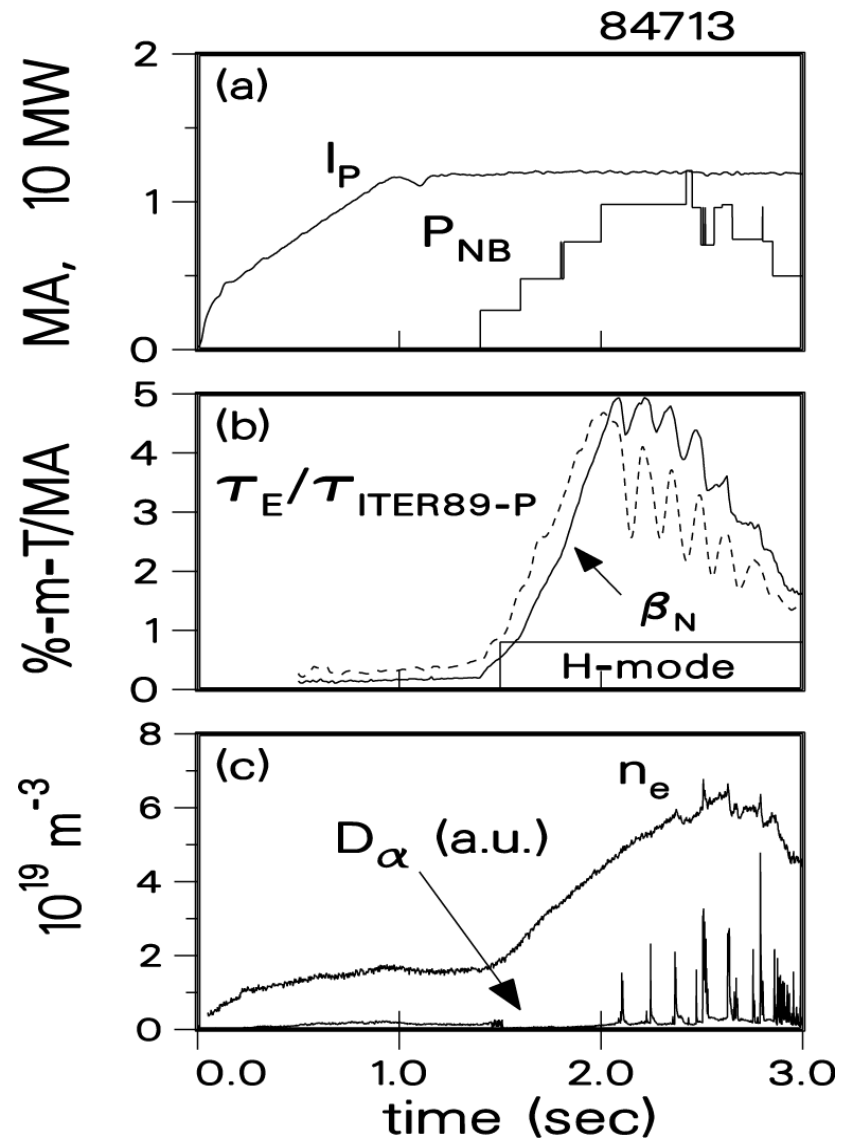
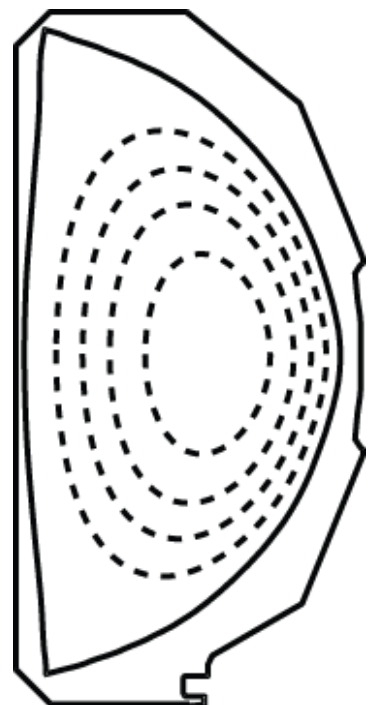
Validation of Magnetic Response Matrix against Vacuum Data Is Extremely Crucial

- DIII-D
- External coils only
- Necessary not sufficient



Magnetic Reconstructions Are Routinely Used To Obtain Plasma Geometry, β , and Confinement Time

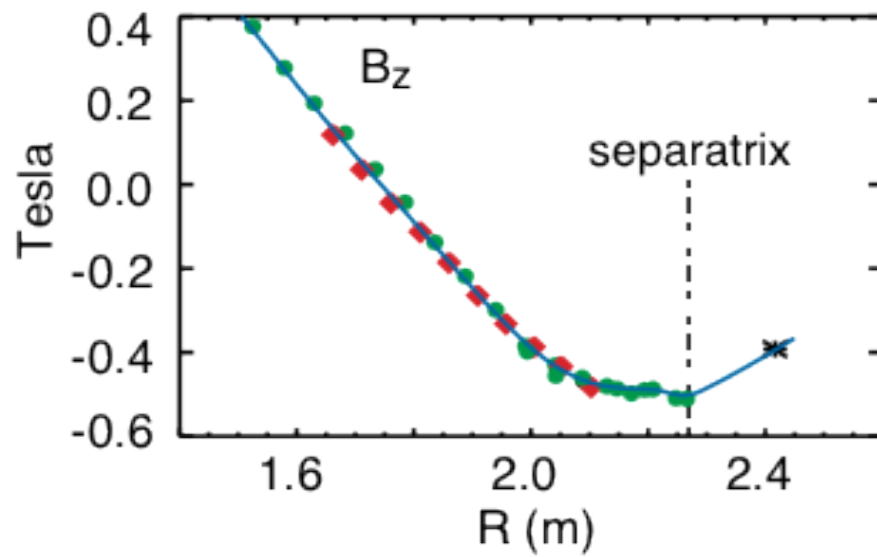
- DIII-D NCS discharge
- External magnetic data only



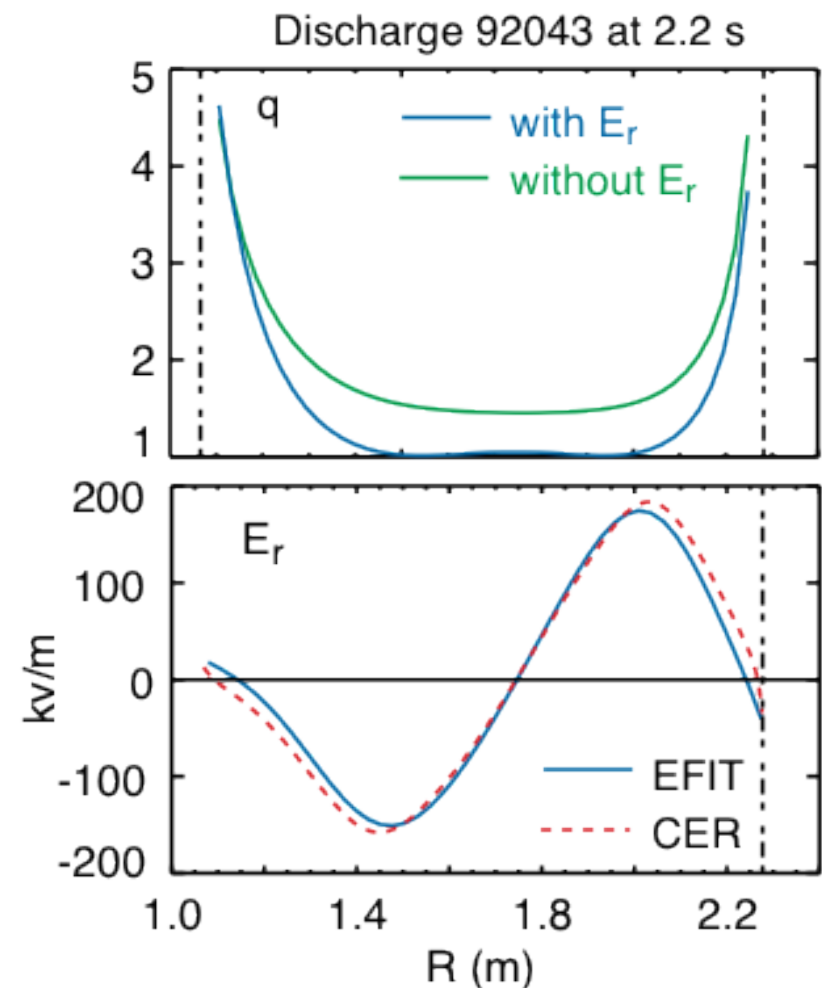
Reconstructed E_R from MSE and Magnetics Agrees Well with E_R Inferred from CER

- MSE with two-viewing angles
- MSE responses are linearized and incorporated into the response matrix

$$\tan \gamma = \frac{A_1 B_Z + A_5 E_R}{A_2 B_\phi + A_3 B_R + A_4 B_Z + A_6 E_Z + A_7 E_R}$$



Rice, Burrell, Lao, Linliu, Phys. Rev. Lett. 79 (1997) 2694



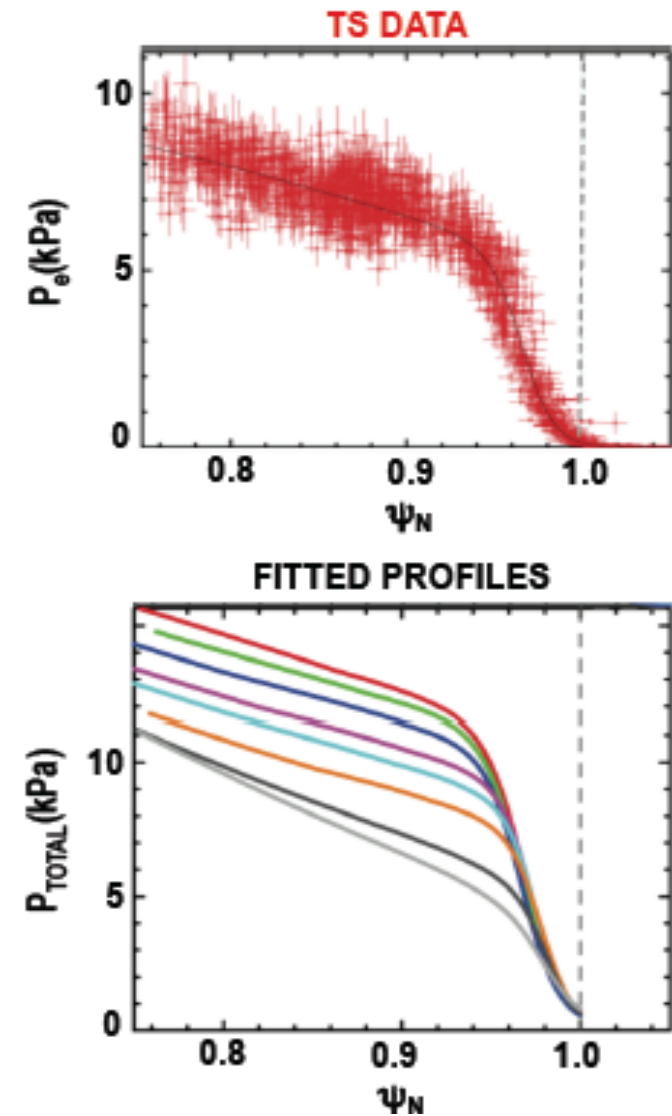
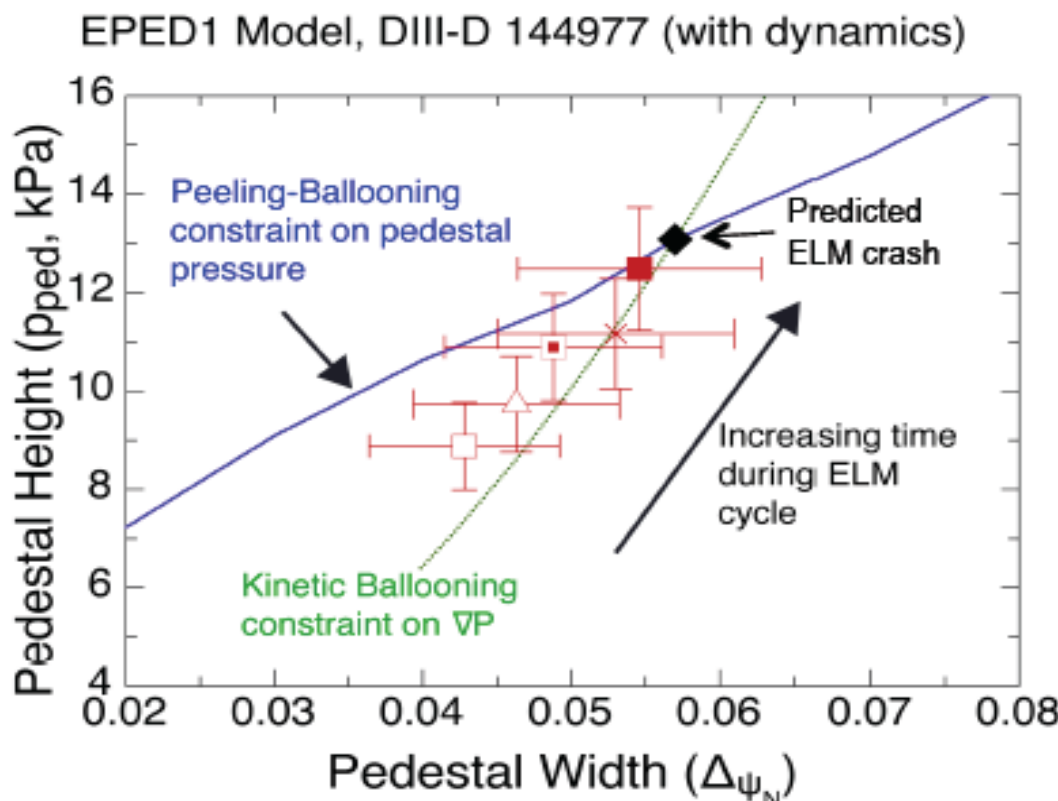
Kinetic EFIT Reconstruction

- Explore discharge using **review+** and **efitviewer**
- Run EFIT with MSE to get G EQDSK
- Run GProfile to map profiles into flux space
- Run ONETWO to get beam and total pressure profile
- Make kinetic EFIT input file

IMFIT/OMFIT Kinetic EFIT
Tools

Kinetic EFIT Reconstruction Is Necessary for Detailed Transport and Stability Analyses

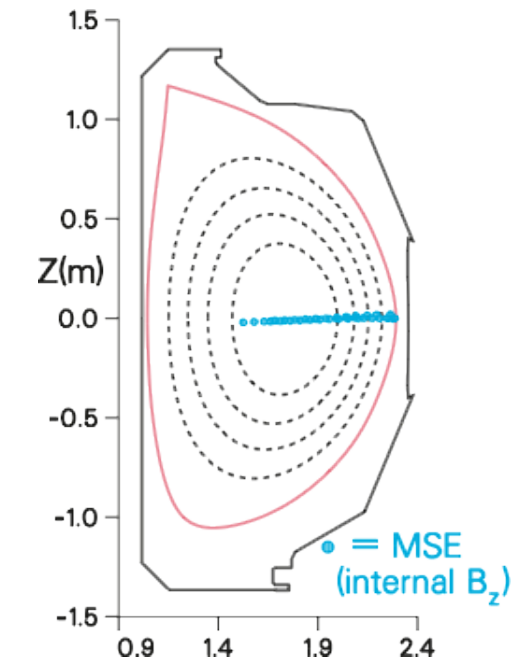
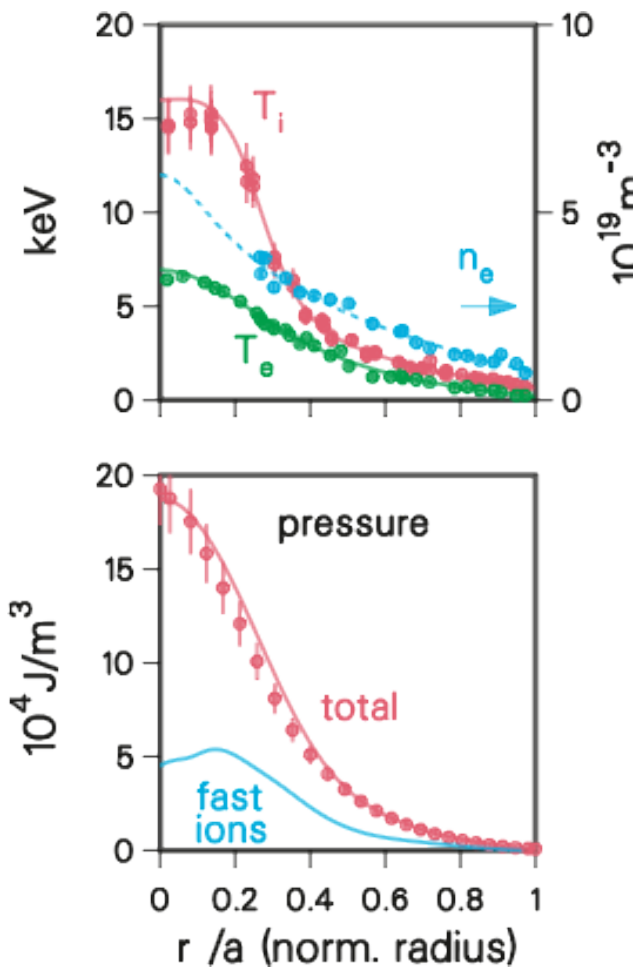
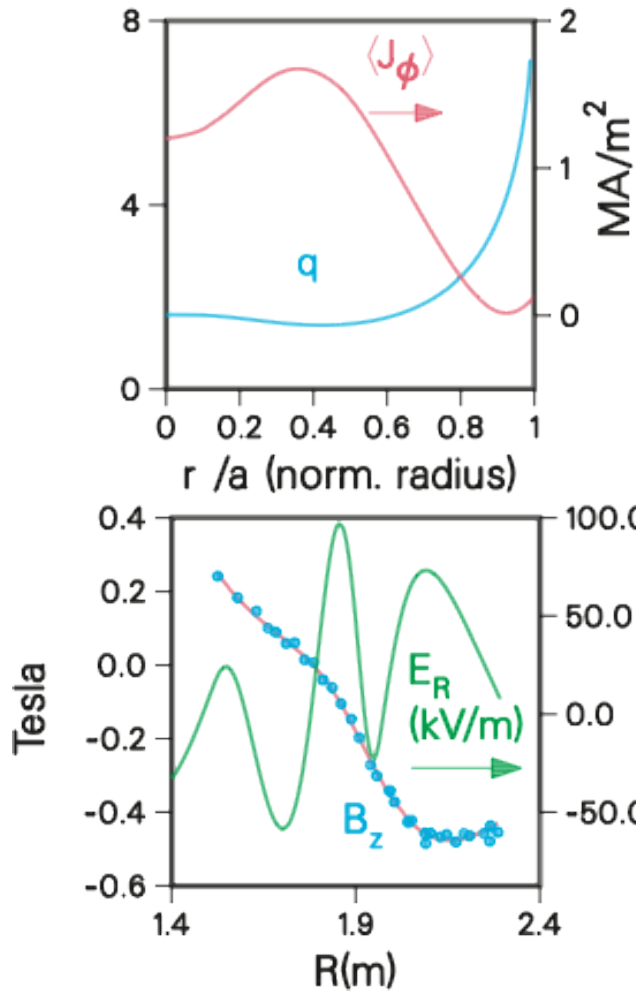
- Recent DIII-D Thomson upgrade allows detailed comparison of profile evolution between ELMs



Snyder 2011 Invited APS; Groebner 2011 APS

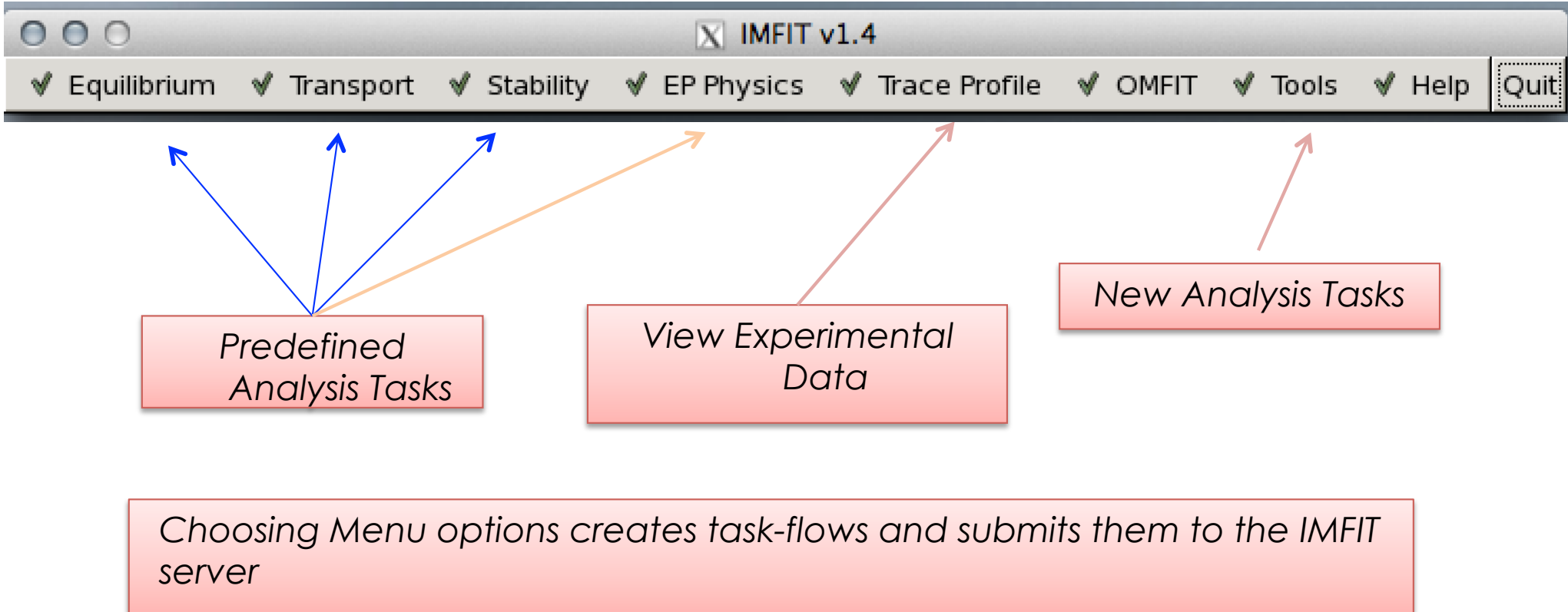
Full Kinetic EFIT Reconstruction Using Magnetic, Kinetic, and MSE Data

Run managed by Equilibrium Manager



IMFIT Equilibrium Reconstruction Tool

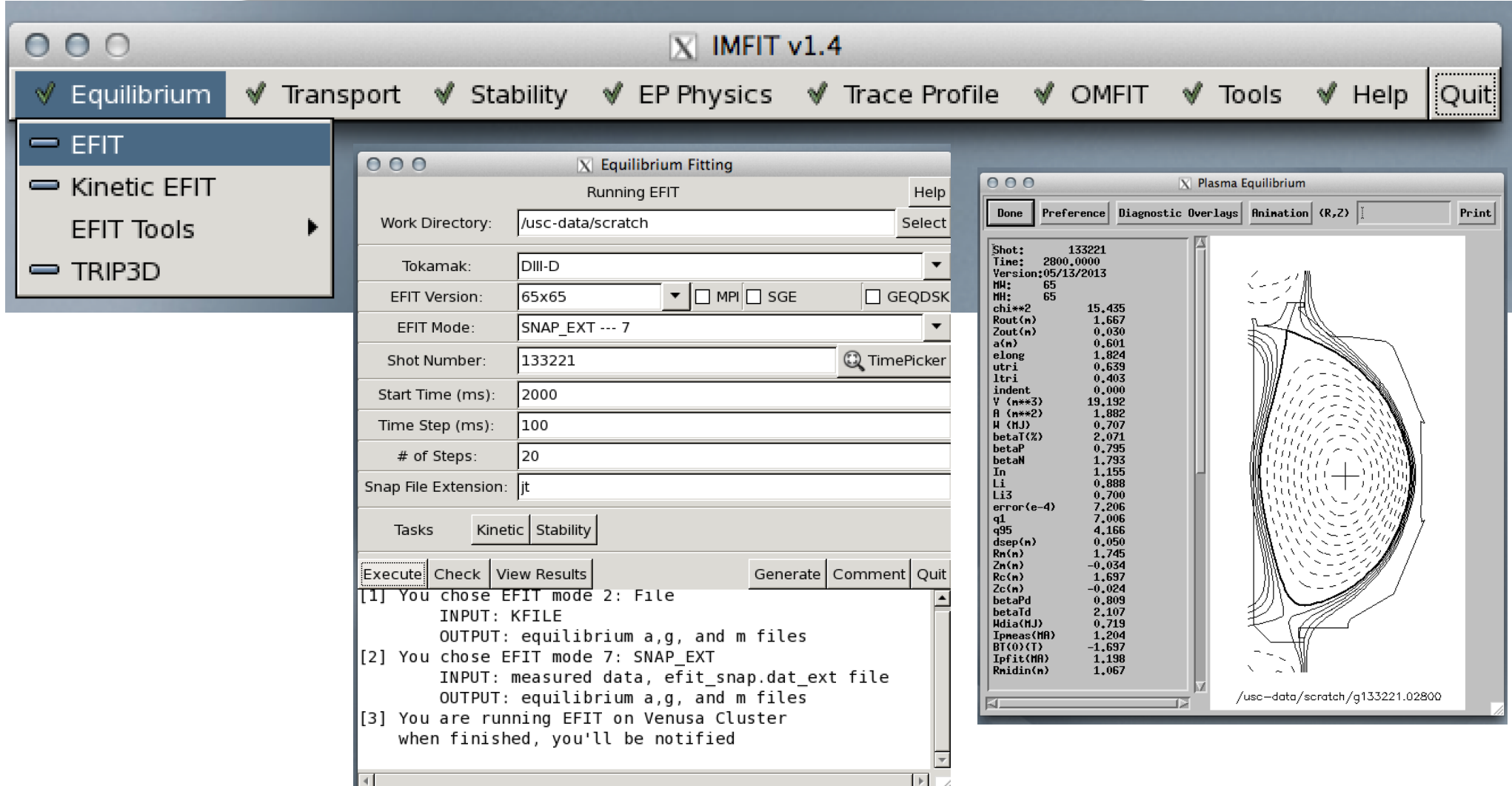
- DIII-D, EAST, and SST-1 (HL-2A, HL-2M, KSTAR)



Based on the public PyGTK graphical user interface toolkit for Python

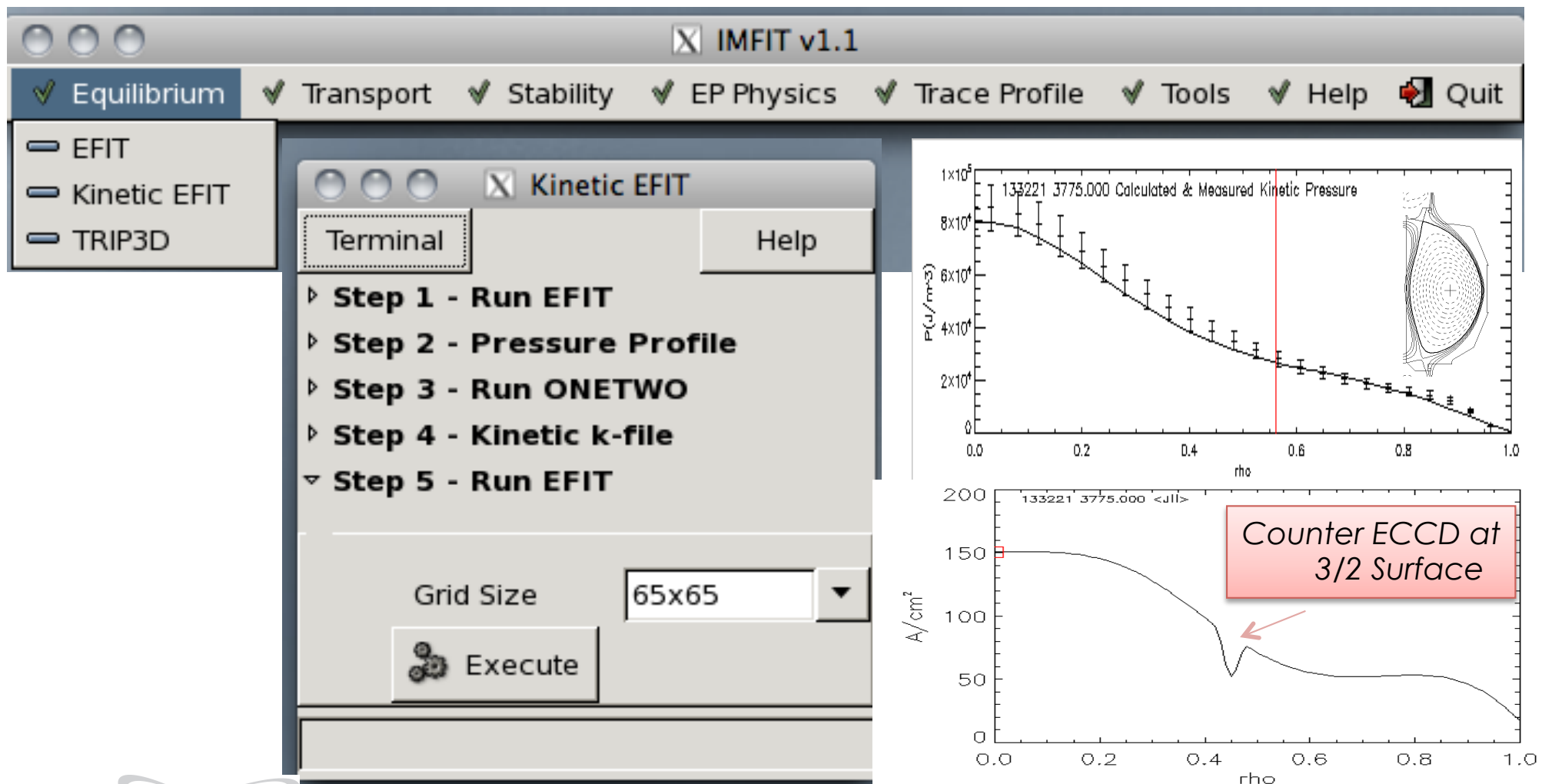
IMFIT EFIT Reconstruction

Run managed by Equilibrium Manager



IMFIT Kinetic EFIT Reconstruction

Run managed by Equilibrium Manager



MHD Stability Applications Have Stringent Equilibrium Requirements

- **Tightly satisfy force balance**
 - Relative error $\varepsilon < 1 \times 10^{-8}$
- **High spatial resolution**
 - 129×129 or higher
- **Sufficiently accurate representation of experimental pressure and current profiles**
 - MSE, kinetic profiles

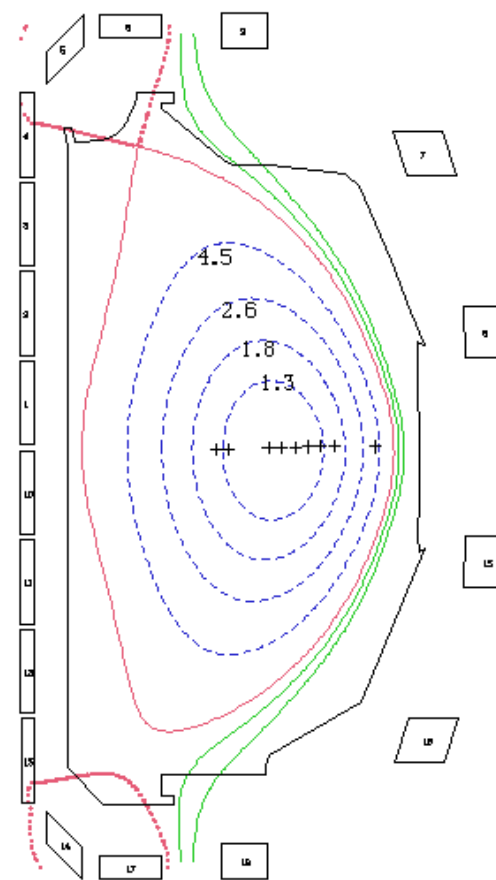
Tight Convergence Could Be Challenging

```

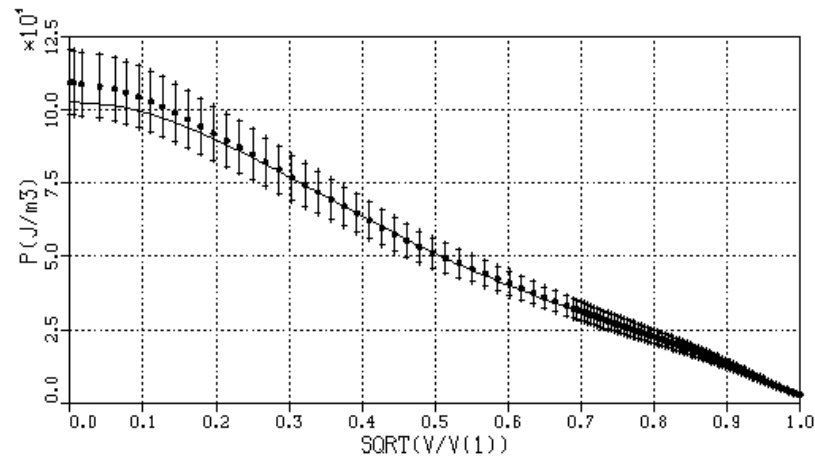
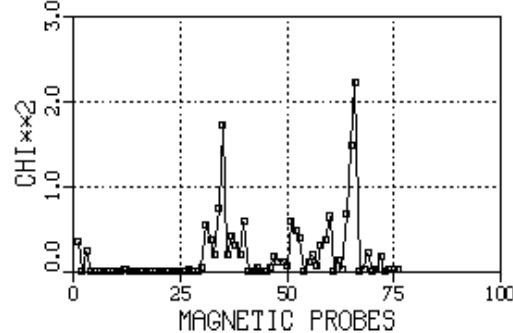
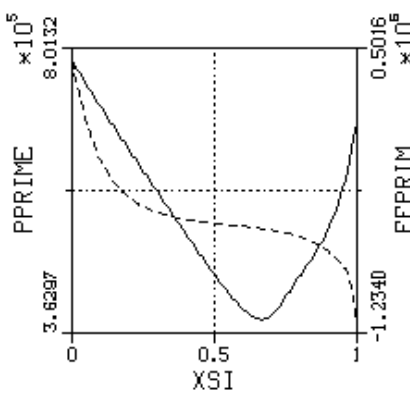
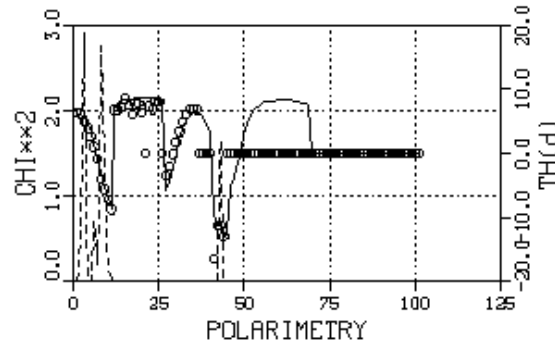
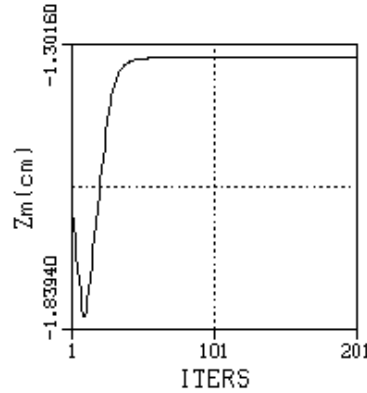
h EFITD129 x129 03/29/2010 k134119.04175_t2ppd
date ran = 25-Jan-11
shot # - 134119
t(ms,us) - 4175 0
chi2(mag) - 2.081E+01
rout(cm) - 166.40
zout(cm) - 3.067
a(cm) - 59.39
elong - 1.876
utri,ltri= 0.64 0.45
indent = 0.000
V,A(lm3,2)= 19.03 1.869
energy(j) - 9.587E+05
betat(%) - 2.84
betap - 2.51
betan,In - 3.66 0.78
li,li3 = 0.93 0.72
error, # = 1.415E-04 201
delstar = 3.5E-01 9.4E-04
ux,lx(cm)= 9.34 13.38
J0n,J1n - 3.88 0.14
q1,q95 - 12.88 7.01
deep(cm) - 5.410
rm,rc(cm)- 180.9 181.7
zm,zc(cm)- -1.33 -0.62
betapd,w = 2.50 0.00
betatd,w = 2.82 0.00
wdia(J) = 9.537E+05
wtor(J) = 0.000E+00
      data used:
lpl(kA) - 798.7
bt0(t) - -1.692
42 flux loops, 0 ECE
48 magnetic probes
  1 rogow 0 fc 0 ec
  0 dl, 9 mse 0 li
scrapof(mm) 20.0 40.0

```

→

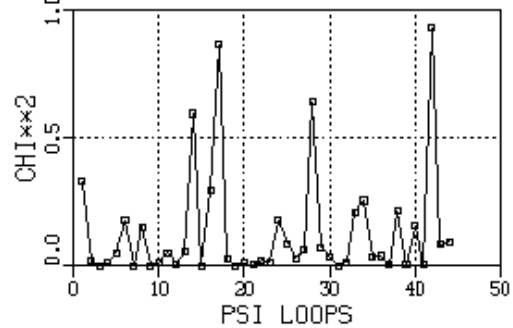


Tight Convergence Could Be Challenging



$\alpha, g =$	1.000	0.541
	2.375	119.800
	0.492	-1.050
	16.362	-24.932
	0.558	-1.478
	-2.111	-681.857
	0.874	
	45.714	

$a_0 = 7.814E+05$
 $cno = 1.401E+04$



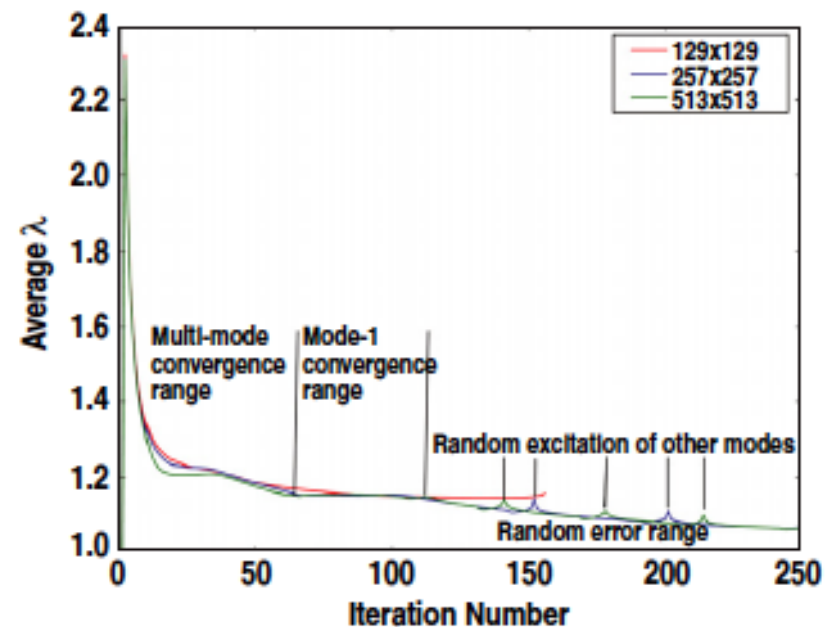
EFIT Iteration Process Can Be Shown Related to the Axisymmetric Stability Problem

- EFIT iteratively solves the GS equation using the Picard's scheme

$$\Delta^* \psi^{m+\theta} = -\mu_0 R J_\phi(R, \psi^m)$$

$$\psi^{m+1} = (1 - \theta) \psi^m + \theta \psi^{m+\theta}$$

$$\varepsilon = \text{Max} \left| \frac{\psi^{m+1} - \psi^m}{\psi_{norm}} \right|_{Grid}$$



- EFIT iteration step equivalent to the variation in the δW expression
- Iteration error is related to the least-stable axisymmetric mode

Two-Stage Approach Provides a Convenient Mean to Compute Equilibria for Stability Applications

- **Free-boundary reconstruction with reasonable convergence**
 - 129×129 , relative error $\varepsilon \sim 1 \times 10^{-4}$
- **Fixed-boundary EFIT equilibrium with given pressure and current profiles P' and FF'**
 - 129×129 or higher, $\varepsilon \sim 1 \times 10^{-8}$
 - G EQDSK as input: Boundary, P' , FF' , limiter

G EQDSK Fixed Boundary EFIT Namelist Input

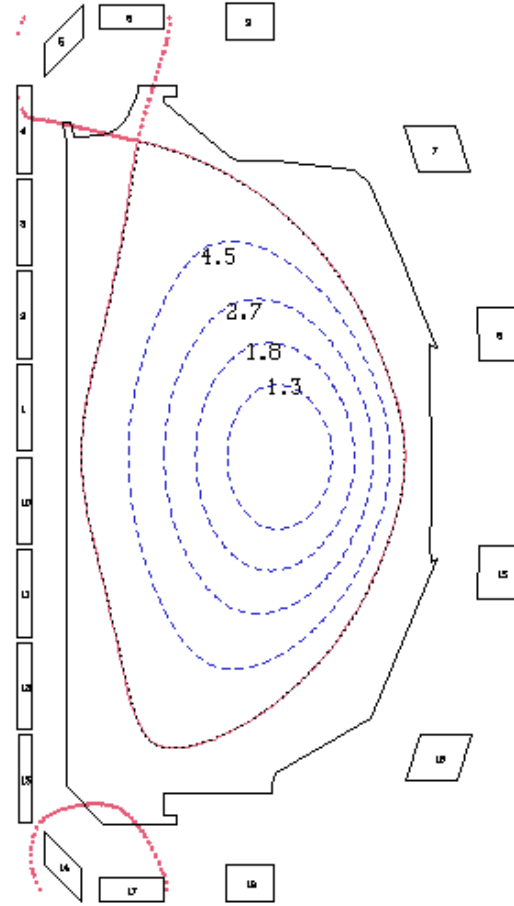
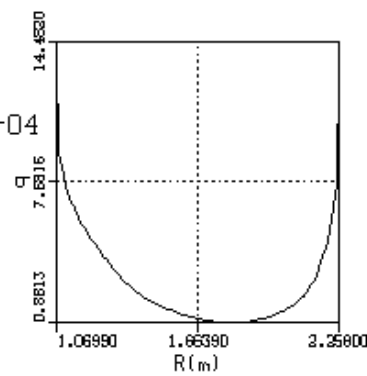
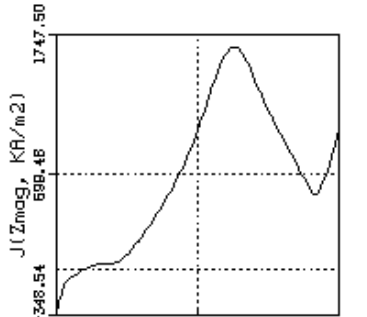
Boundary, P', FF', Limiter

```
Terminal — ssh — 100x24
r134119.04176_fixs 24 Lines

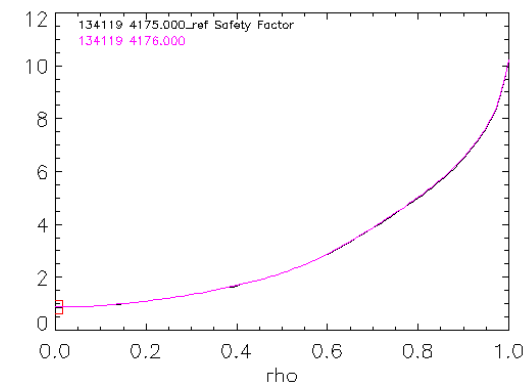
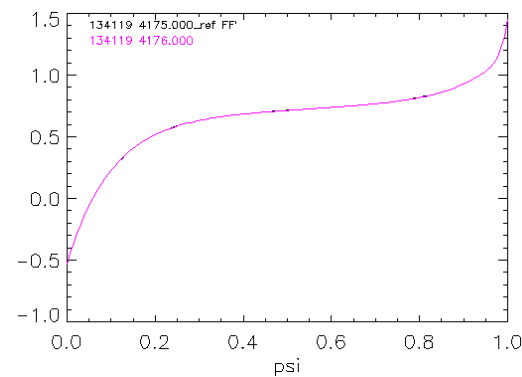
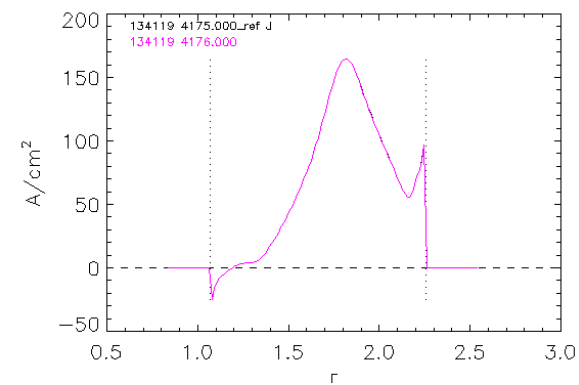
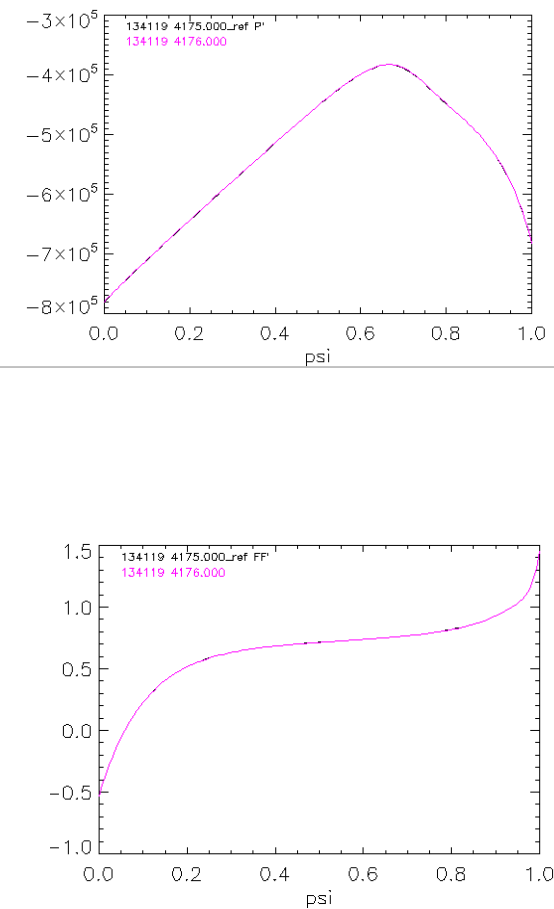
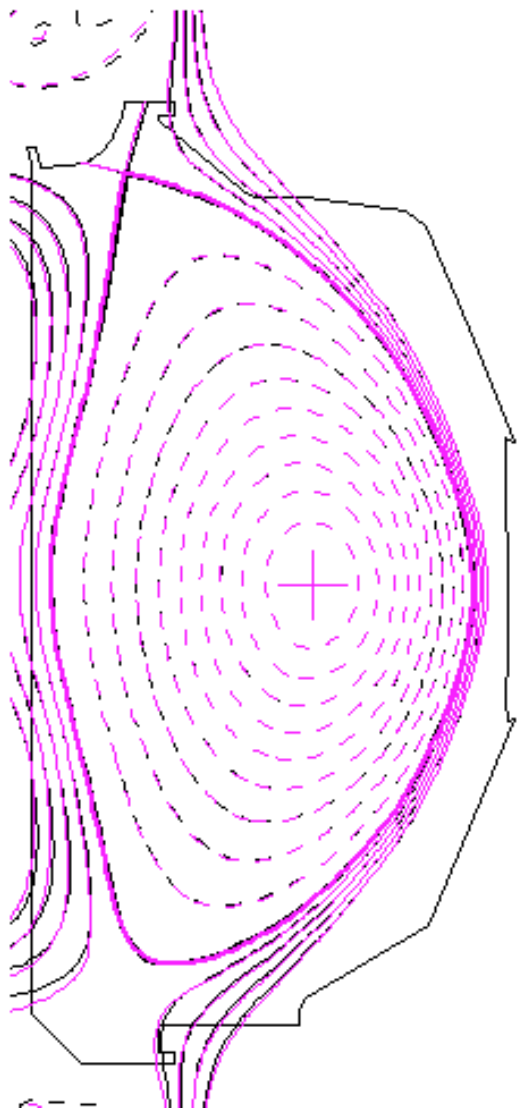
♦
&IN1
ISHOT = 134119
ITIME = 4176
PLASMA = 793831.9
BTOR = -1.69236
RCENTR = 1.6955
IFREF=4 PSIBRY = 2.25939E-02
IECURR=1
ECURRT = -2757.12, -2733.01, -2710.17, -2711.63, -2692.21, -2689.36
ERROR = 1.00000E-08 RELAX=1.00
MXITER = 1 NXITER=-100
FWTBDRY = 10.0 1.0 1.0 1.0 1.0 1.0 1.0 1.0 1.0 1.0 1.0 1.0 1.0 1.0 1.0 1.0
1.0 10.0 1.0 1.0 1.0 1.0 1.0 1.0 1.0 1.0 1.0 1.0 1.0 1.0 1.0 1.0 1.0
1.0 1.0 1.0 1.0 1.0 1.0 1.0 1.0 1.0 1.0 1.0 1.0 1.0 1.0 10.0 1.0 1.0
1.0 1.0 1.0 1.0 1.0 1.0 1.0 1.0 1.0 1.0 1.0 1.0 1.0 1.0 1.0 1.0 1.0
1.0 1.0 1.0 1.0 1.0 10.0 1.0 1.0 1.0 1.0 1.0 1.0 1.0 1.0 1.0 1.0 1.0
1.0 1.0 1.0 1.0 1.0 1.0 0.0 0.0 0.0 0.0 0.0 0.0 0.0 0.0 0.0 0.0 0.0
0.0 0.0 0.0 0.0 0.0 0.0 0.0 0.0 0.0 0.0 0.0 0.0 0.0 0.0 0.0 0.0 0.0
/
&PROFILE_EXT
GEQDSK_EXT='g134119.04175_ref'
SCALEPP_EXT = 1.0    SCALEFFP_EXT = 1.0
/
```

Fixed Boundary Equilibrium from G EQDSK Allows a Tighter Convergence

```
b EFITD129 x129 01/14/2011 r134119.04176_flx
date ran = 26-Jan-11
shot # - 134119
t(ms,us) - 4176 0
chi2(mag) - 0.000E+00
rout(cm) - 166.39
zout(cm) - 3.244
a(cm) - 59.41
elong - 1.876
utri,ltri= 0.65 0.43
indent = 0.000
V,A(m3,2)- 19.08 1.874
energy(j)- 9.589E+05
betat(%) - 2.83
betap - 2.51
betan,In - 3.65 0.77
li,li3 = 0.93 0.72
error, # = 8.292E-09 27
delstar = 8.2E-08 7.2E-04
ux,Lx(cm)= 8.70 12.89
J0n,J1n - 3.89 0.13
q1,q95 - 13.87 7.07
deep(cm) - 5.374
rm,rc(cm)- 180.9 181.6
zm,zc(cm)- -1.32 -0.58
betapd,w = 1.31 0.00
betad,w = 1.48 0.00
wdia(J) = 5.014E+05
wtor(J) = 0.000E+00
    data used:
lp(ka) - 793.8
bt0(t) - -1.692
0 flux loops, 0 ECE
0 magnetic probes
0 rogov 0 fc 0 ec
lcp, lvs= 0 0
kf, kp, E= 4 4 0
fpd, p, E- 0.0 0.0 0.0
fwbp, fwq- 0.0 0.0
Zel(cm) - 0.000
```



Fixed and Free Boundary Equilibria Agrees



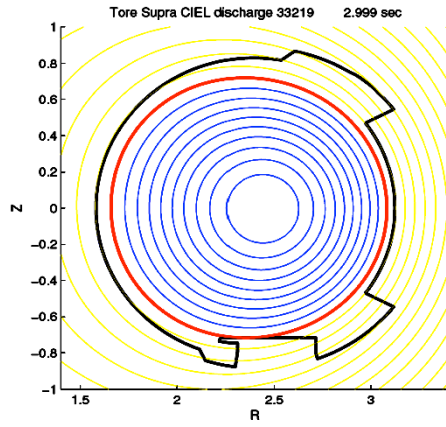
Many Progresses Have Been Made toward Development of a Single EFIT Version for Different Tokamaks

- EU IM EFIT efforts
- Utilize ITM data structures

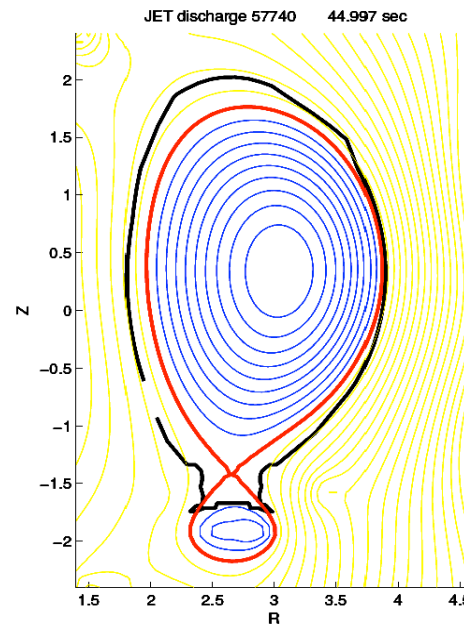
Appel, et al. EPS 2006

EFIT++

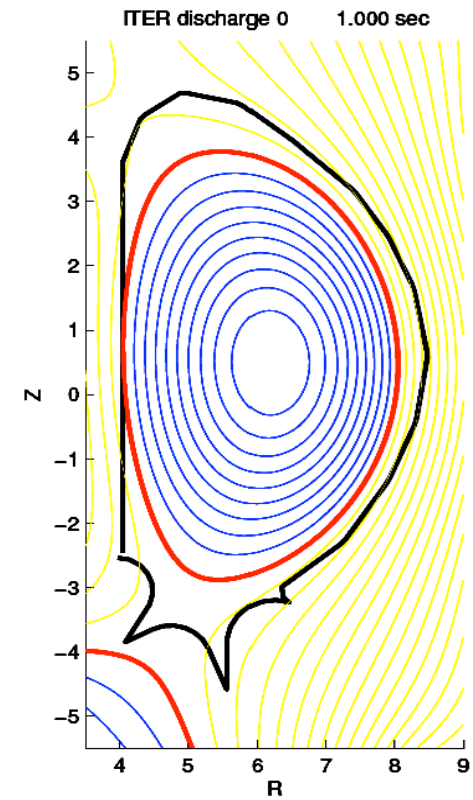
TORE-SUPRA



JET



ITER



New EFIT Developments: 3D Extension

- **3D extension to account for intrinsic non-axisymmetric error or externally applied perturbation magnetic fields and toroidal field ripple**

- V3FIT project (EFIT response + VMEC 3D). Nested flux surfaces.

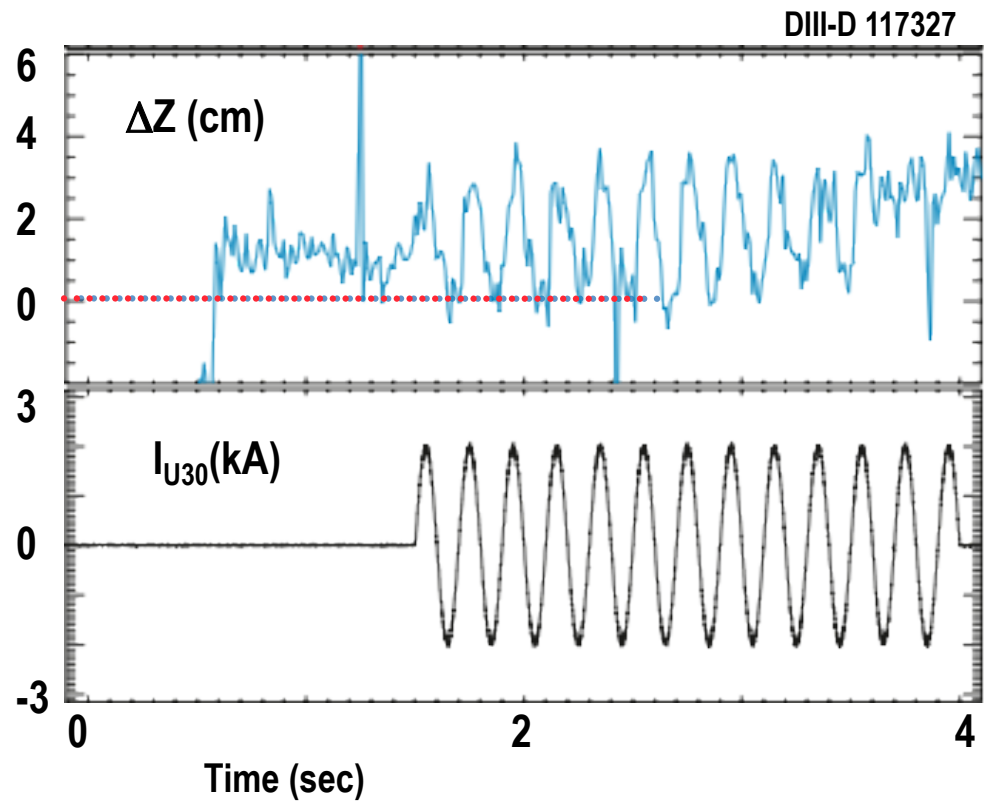
[Hirshman, Lazarus, Hanson, Knowlton, Lao, Phys. Plasmas 11 (2004) 595]

[Hanson, Hirshman, Knowlton, Lao, Lazarus, Shields Nucl. Fusion 49 (2009) 075031

- 3D EFIT extension based on a perturbation approach with allowance for island structure and magnetic stochasticity

Sestero Plasma Phys. 15 (1973) 709

Recent DIII-D I-Coil RMP modulation experiments indicate perturbation fields can have a large effect on separatrix locations

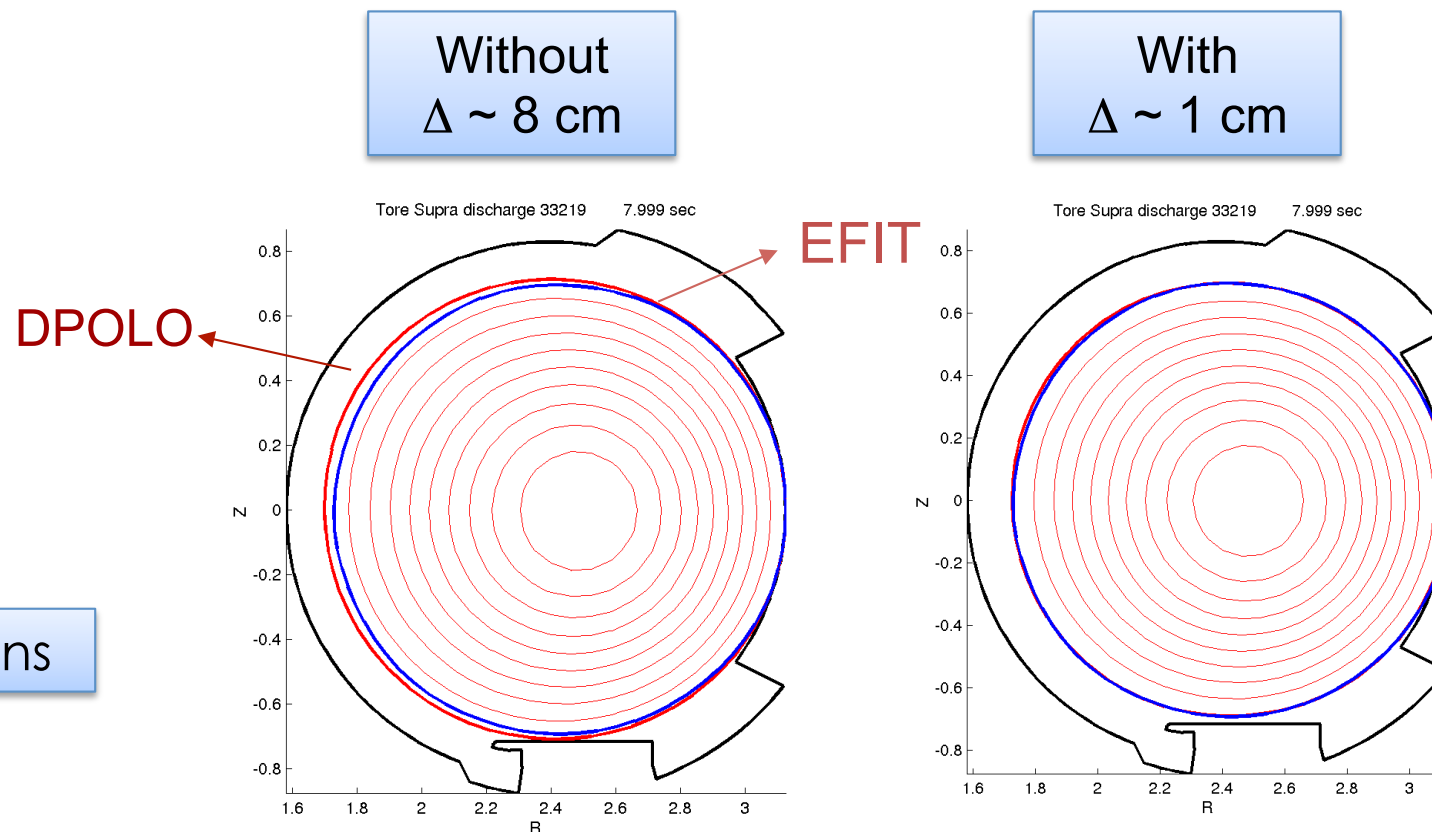


Lao, et al. APS 2005

Perturbation Technique To Include 3D Perturbation Magnetic Fields in EFIT Looks Promising

correction for 3D toroidal field ripple in EFIT is essential for TORE-SUPRA

RMP Applications



Zwingmann, et al. EPS 2005

Lao/ EFIT May 2013



cea

EFIT Related Publications: 1985 – 2013

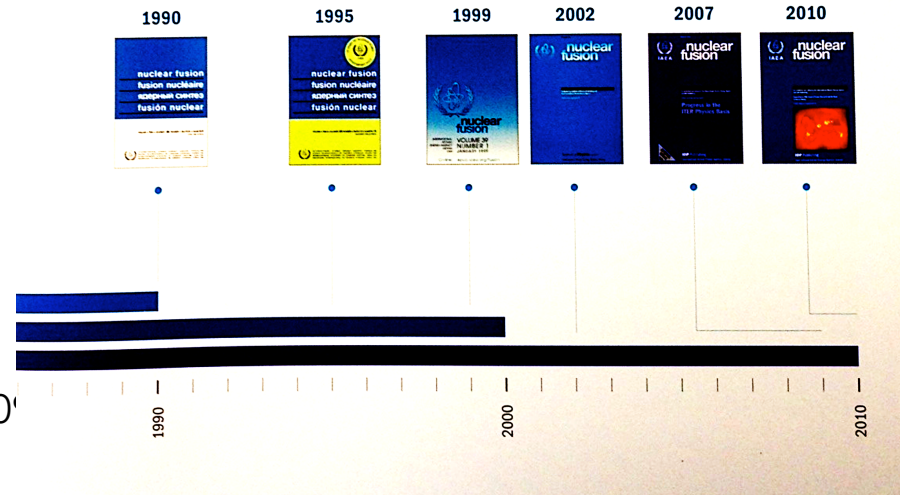
<https://fusion.gat.com/theory/Efit>

- Lao et al., Nucl. Fusion 25 (1985) 1421
Lao et al., Nucl. Fusion 25 (1985) 1611
Lao et al., Nucl. Fusion 30 (1990) 1035
Lao et al., Nucl. Fusion 31 (1991) 1909
O'Brien et al., Nucl. Fusion 32 (1992) 1351
Nelson et al., Phys. Rev. Lett. 72 (1994) 3666
Forest et al., Phys. Rev. Lett. 73 (1994) 2444
Rice et al., Phys. Rev. Lett. 79 (1997) 2694
Ferron et al., Nucl. Fusion 38 (1998) 1005
Lee et al., Fusion Technol. 36 (1999) 278
Appel et al., Nucl. Fusion 41 (2001) 169
Lao et al. AIP Conf. Proc. 595 (2001) 310
Sabbagh et al., Nucl. Fusion 41 (2001) 1601
Peng et al., Fusion Eng. Des. 60 (2002) 319
Zwingmann et al., Nucl. Fusion 43 (2003) 842
Li et al., Phys. Plasmas 10 (2003) 1653
Lao et al., Fusion Sci. Tech. 48 (2005) 968
Qian et al., Nucl. Fusion 49 (2009) 025003
Qian et al., Plasma Sci. Technol. 11 (2009) 142
Qian et al., Chinese Phys. B. 18 (2009) 1172
Ren et al., Plasma Phys. Control. Fusion 53 (2011) 095001
Yue et al., Plasma Phys. Control. Fusion 55 (2013)

Nuclear Fusion 1960 2011 Archive

Since its inception, *Nuclear Fusion* has been supported by the leading scientists in the field and has published some of the most important papers in fusion research. A small sample includes:

- M. N. Rosenbluth, R. Z. Sagdeev, J. B. Taylor et al 1966 Destruction of magnetic surfaces by magnetic field irregularities
- H. P. Furth 1975 Tokamak research
- T. H. Stix 1975 Fast-wave heating of a two-component plasma
- M. N. Rosenbluth and M. N. Bussac 1979 MHD stability of spheromaks
- G. M. McCracken, P E Stott 1979 Plasma-surface interactions in tokamaks
- S. P. Hirshman, D. J. Sigmar 1981 Neoclassical transport of impurities in tokamak plasmas
- J. Meyer-ter-Vehn 1982 On energy gain of fusion targets: the model of Kidder and Bodner improved
- P. C. Liewer 1985 Measurements of microturbulence in tokamaks and comparisons with theories of turbulence and anomalous transport
- L. L. Lao, H. St. John, R. D. Stambaugh et al 1985 Reconstruction of current profile parameters and plasma shapes in tokamaks
- M. Kikuchi 1990 Steady state tokamak reactor based on the bootstrap current



Summary

- Equilibrium reconstruction is an important component of tokamak data analysis and modeling
- EFIT reconstruct 2D tokamak equilibrium by solving the GS equation while approximately conserving experimental measurements
- EFIT efficiently searches for the solution vector by transforming the nonlinear optimization problem into a sequence of linear problems using a response function formalism and a Picard algorithm
- Amount of reconstructed information increases with diagnostic measurements available for reconstruction
- Internal current and kinetic profile measurements are necessary for full equilibrium reconstruction
- Proper choice of basis functions, boundary conditions, and physics constraints are essential to allow accurate reconstructions
- Current developments include use of GPU to speed up the computations and 3D extension to reconstruct perturbed equilibrium